Second Order Task Specifications in the Geometric Design of Spatial Mechanical Linkages

Nina P. Robson, Texas A&M University; J. Michael McCarthy, University of California, Irvine

Abstract

This paper builds on the authors' planar kinematic synthesis for contact task specifications and formulates the kinematic specification of the synthesis problem for spatial open-serial chains in which a desired acceleration of the end-effector is specified.

Applications of this research focus on the design of spatial linkages to maintain specified local motion. A recently developed failure recovery strategy of a general six-degree-of-freedom TRS robotic arm is discussed and some experimental set up and tests of the proposed failure recovery are presented. The authors also briefly show another possible application of the geometric design of linkages using acceleration task specifications. It combines the second-order effects of the task with the particular kinematics of the chain to yield free parameters that allow for more than one system to accomplish one and the same task.

Introduction

This study considered the synthesis of spatial chains to guide an end-effector through a number of multiply separated positions [1], [2]. The kinematic specification is a number of task positions with specified end-effector velocities and accelerations. The goal of this study was to obtain all of the solutions to a given task specification in order to design mechanical linkages that could move the end-effector smoothly through the specified task. Research in the synthesis of serial chains to achieve acceleration requirements is limited. It is primarily found in the synthesis theory for planar RR chains, and the work by Chen and Roth [3] for spatial chains. The use of second-order effects first appeared in the analysis of grasping in a work by Hanafusa and Asada [4], where planar objects are grasped with three elastic rods.

Cai and Roth [5] and Montana [6] developed an expression for the velocity of the point of contact between two rigid bodies that includes the curvature of the contact bodies. Second-order contact kinematics for regular contacts such as surface-surface, curve-curve, curve-surface and vertex-surface are formulated in a unified framework in the recent work of Park et al. [7], extending Montana's first-order contact kinematics for surface-surface contact only. Sarkar et al. [8] develop an expression for the acceleration of the contact point between two contacting bodies.

Second-order considerations have also appeared in work by Trinkle [9] in the study of stability of frictionless polyhedral objects in the presence of gravity. The mobility of bodies in contact has been studied using first-order theories that are based on notions of instantaneous force and velocities [10]. For example, Ohwovoriole and Roth [10] describe the relative motion of contacting bodies in terms of Screw Theory, which is a first-order theory. Using first-order notions, Reuleaux [11], Mishra et al. [12] and Markenskoff et al. [13], derive bounds on the number of frictionless point contacts required for force closure, which is one means of immobilizing an object. However, first-order theories are inadequate in practice. The source of deficiency is that the relative mobility of an object in contact with finger bodies is not an infinitesimal notion but a local one. One must consider the local motions of the object, not the tangential aspects of the motions, as employed by the first-order theories.

Rimon and Burdick [14], [15] show that acceleration properties of movement can be used to effectively constrain a rigid body for part-fixturing and grasping applications. In previous work by the authors, planar synthesis [16] was presented as a technique for deriving geometric constraints on position, velocity and acceleration from contact and curvature task requirements. These constraints yielded design equations that can be solved to determine the dimensions of the serial chain.

In this current study, the authors briefly present this planar approach, expand on the spatial approach [17], [18] and present some of the applications of second-order task specifications for the geometric design of spatial linkages.

Geometric Design of Planar Mechanical Linkages with Task Acceleration Specifications

Assume that the planar task consists of positioning an end-effector of a robot arm at a start and a finish position M^j, j=1,…, n, such that in these positions there are prescribed velocities and accelerations. Let the movement of a rigid body be defined by the parameterized set of 3 x 3 homogeneous transforms $[\mathbf{T}(t)]=[R(t), \mathbf{d}(t)]$ constructed from a rotation matrix, R(t), and translation vector $\mathbf{d}(t)$. A point $\mathbf{p}$ fixed in the moving body traces a trajectory $\mathbf{P}(t)$ in a fixed coordinate frame F such that:

$$\begin{Bmatrix} P_x(t) \\ P_y(t) \\ 1 \end{Bmatrix} = \begin{bmatrix} \cos\phi(t) & -\sin\phi(t) & d_x(t) \\ \sin\phi(t) & \cos\phi(t) & d_y(t) \\ 0 & 0 & 1 \end{bmatrix} \begin{Bmatrix} p_x \\ p_y \\ 1 \end{Bmatrix}, \quad (1)$$

or

$$\mathbf{P}(t) = [T(t)]\mathbf{p}. \quad (2)$$

The goal is to determine the movement of the end-effector as defined by [**T**(t)].

The movement of M relative to a world frame F in the vicinity of a reference position, defined by t=0, can be expressed by the Taylor series expansion,

$$[T^j(t)] = [T_0^j] + [T_1^j]t + \frac{1}{2}[T_2^j]t^2 + \ldots, \; j = 1, \ldots, n$$
$$\text{where} \quad [T_i^j] = \frac{d^i[T^j]}{dt^i}\Big|_{t=0}. \quad (3)$$

The matrices $[T_0^j]$, $[T_1^j]$ and $[T_2^j]$ are defined by the position, velocity and acceleration of the end-effector in the vicinity of each task position M^j. Therefore, a point **p** in M has the trajectory **P**(t) defined by the equation

$$\mathbf{P}^j(t) = [T^j(t)]\mathbf{p} = [T_0^j + T_1^j t + \frac{1}{2}T_2^j t^2 + \ldots]\mathbf{p}. \quad (4)$$

Let $\mathbf{p}=[T_0^j]^{-1}\mathbf{P}$, which yields

$$\mathbf{P}^j(t) = [T_0^j + T_1^j t + \frac{1}{2}T_2^j t^2 + \cdots][T_0^j]^{-1}\mathbf{P}^j,$$
$$= [I + \Omega^j t + \frac{1}{2}\Lambda^j t^2 + \cdots]\mathbf{P}^j, \quad (5)$$

where

$$[\Omega^j] = \begin{bmatrix} 0 & -\phi_1 & d_{x1} + d_{x0}\phi_1 \\ \phi_1 & 0 & d_{y1} - d_{x0}\phi_1 \\ 0 & 0 & 0 \end{bmatrix}, \quad [\Lambda^j] = \begin{bmatrix} -\phi_1^2 & -\phi_2 & d_{x2} + d_{x0}\phi_1^2 + d_{y0}\phi_2 \\ \phi_2 & -\phi_1^2 & d_{y2} + d_{y0}\phi_1^2 - d_{x0}\phi_2 \\ 0 & 0 & 0 \end{bmatrix} \quad (6)$$

are the planar velocity and planar acceleration matrices, which are defined by the end-effector velocity and acceleration specifications in the vicinity of some task positions M^j, j=1, ..., n.

For example, the design parameters for a planar RR chain are the coordinates $\mathbf{B}=(B_x, B_y)$ of the fixed pivot, the coordinates $\mathbf{P}^1=(P_x, P_y)$ of the moving pivot when the floating link is in the first position, and the length R of the link. In each task position the moving pivot $\mathbf{P}^j$ is constrained to lie at the distance R from **B**, so we have,

$$(\mathbf{P}(t) - \mathbf{B}) \cdot (\mathbf{P}(t) - \mathbf{B}) = R^2. \quad (7)$$

The first and second derivative of this equation provide the velocity constraint equation

$$\frac{d}{dt}\mathbf{P} \cdot (\mathbf{P} - \mathbf{B}) = 0, \quad (8)$$

and the acceleration constraint equation

$$\frac{d^2}{dt^2}\mathbf{P} \cdot (\mathbf{P} - \mathbf{B}) + (\frac{d}{dt}\mathbf{P}) \cdot (\frac{d}{dt}\mathbf{P}) = 0. \quad (9)$$

In order to determine the five design parameters, five design equations are required. Choosing one of the task positions to be the first and using the relative displacement matrices $[D_{1j}] = [T_0^j][T_0^1]^{-1}$ allow one to define coordinates $\mathbf{P}^j$ taken by the moving pivot as follows:

$$\mathbf{P}^j = [D_{1j}]\mathbf{P}^1. \quad (10)$$

It is now possible to substitute $\mathbf{P}^j$ in equation (7) to obtain

$$([D_{1j}]\mathbf{P}^1 - \mathbf{B}) \cdot ([D_{1j}]\mathbf{P}^1 - \mathbf{B}) = R^2, \quad i = 1, \ldots, n. \quad (11)$$

These are the position design equations. Notice that $[D_{11}]$ is the 3 x 3 identity matrix. From our definition of the 3 x 3 velocity matrix, we have $\frac{d}{dt}\mathbf{P}^j = [\Omega_j][D_{1j}]\mathbf{P}^1$ and substituting $\mathbf{P}^j$ into (8), we obtain the velocity design equations

$$([\Omega^j][D_{1j}]\mathbf{P}^1) \cdot ([D_{1j}]\mathbf{P}^1 - \mathbf{B}) = 0, \quad j = 1, \ldots, n. \quad (12)$$

From our definition of the 3 x 3 acceleration matrix, we have $d^2/dt^2(\mathbf{P}^j) = [\Lambda_j][D_{1j}]\mathbf{P}^1$ and substituting $\mathbf{P}^j$ in equation (9) yields

$$([\Lambda_j][D_{1j}]\mathbf{P}^1) \cdot ([D_{1j}]\mathbf{P}^1 - \mathbf{B}) + ([\Omega^j][D_{1j}]\mathbf{P}^1) \cdot ([\Omega^j][D_{1j}]\mathbf{P}^1) = 0, \quad (13)$$

where j=1,…., n. These are the acceleration design equations. Thus, for each of the n task positions, the position, velocity and acceleration design equations have the following form:

$$\mathcal{P}_j : ([D_{1j}]\mathbf{P}^1 - \mathbf{B}) \cdot ([D_{1j}]\mathbf{P}^1 - \mathbf{B}) = R^2,$$
$$\mathcal{V}_j : ([\Omega^j][D_{1j}]\mathbf{P}^1) \cdot ([D_{1j}]\mathbf{P}^1 - \mathbf{B}) = 0,$$
$$\mathcal{A}_j : ([\Lambda^j][D_{1j}]\mathbf{P}^1) \cdot ([D_{1j}]\mathbf{P}^1 - \mathbf{B})$$
$$+ ([\Omega_j][D_{1j}]\mathbf{P}^1) \cdot ([\Omega_j][D_{1j}]\mathbf{P}^1) = 0, j = 1, \ldots, n. \quad (14)$$

The algebraic solution to the set of four bilinear equations for an RR chain is presented in McCarthy [19] for the case of five position synthesis and applies without any changes to the design equations (14).

Geometric Design of Spatial Mechanical Linkages with Task Acceleration Specifications

Assume that the spatial task consists of positioning an end-effector of a robot arm at a start and a finish position M^j, j=1,...,n, such that in these positions there are prescribed velocities and accelerations. The rotation angles used to define the orientation of the moving body in space are chosen to be (θj, Φj, Ψj), representing the longitude, latitude, and roll angles that position the z-axis of the moving frame in the j-th position. Thus, the rotation matrix $[A^j]$ is given by

$$[A^j] = [Y(\theta_j)][X(-\phi_j)][Z(\psi_j)], \qquad (15)$$

where [X(.)], [Y(.)], and [Z(.)] represent rotations about the x, y and z axes, respectively. Using this convention, and the notation $\mathbf{d}^j=(d_{x,j}, d_{y,j}, d_{z,j})$, the position data can be expressed as the 4 x 4 homogeneous transform

$$[K(t)] = \begin{bmatrix} c\phi c\psi - s\phi s\theta s\psi & -c\psi s\phi s\theta - c\phi s\psi & c\theta s\phi & d_x \\ c\psi s\theta & c\theta c\psi & s\theta & d_y \\ c\psi s\phi - c\phi s\theta s\psi & -c\phi c\psi s\theta + s\phi s\psi & c\phi c\theta & d_z \\ 0 & 0 & 0 & 1 \end{bmatrix}, \qquad (16)$$

where sin(.) and cos(.) are noted with s(.) and c(.), respectively. Let the movement of the task frame M relative to the world frame F be defined by the 4 x 4 homogeneous transform [K(t)], and consider its Taylor series expansion in the vicinity of both start and finish positions, such that

$$[K^j(t)] = [K_0^j] + [K_1^j]t + \frac{1}{2}[K_2^j]t^2 + \ldots, \; j = 1, \ldots, n$$

$$\text{where} \quad [K_i^j] = \frac{d^i[K^j]}{dt^i}\Big|_{t=0}. \qquad (17)$$

The matrices $[\boldsymbol{K}_0^j]$, $[\boldsymbol{K}_1^j]$ and $[\boldsymbol{K}_2^j]$ are defined by the position, velocity and acceleration of the end-effector in the vicinity of the two task positions M^j. A point **p** in the moving frame has the trajectory $\mathbf{P}^j(t)$ in the fixed frame **F** in the vicinity of a task position M^j (see Figure 1), given by the equation

$$\mathbf{P}^j(t) = [K^j(t)]\mathbf{p} = [K_0^j + K_1^j t + \frac{1}{2}K_2^j t^2 + \ldots]\mathbf{p}. \qquad (18)$$

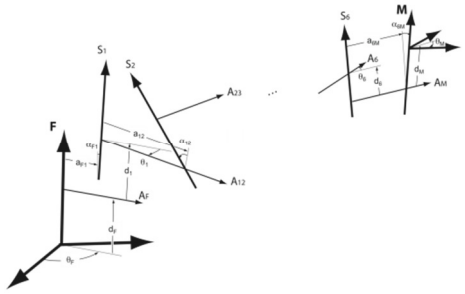

Figure 1. A spatial 6R serial chain with its fixed F and moving M frames

This equation can be rewritten by substituting $\mathbf{p}=[\boldsymbol{K}_0^j]^{-1}\,\mathbf{P}^j$ to obtain the relative transformation

$$\mathbf{P}^j(t) = [K_0^j + K_1^j t + \frac{1}{2}K_2^j t^2 + \cdots][K_0^j]^{-1}\mathbf{P}^j,$$
$$= [I + \Omega^j t + \frac{1}{2}\Lambda^j t^2 + \cdots]\mathbf{P}^j. \qquad (19)$$

The kinematic specification consists of set of spatial displacements and the associated angular and linear velocities $[V^j]=[W^j, \mathbf{v}^j]$, j=1, ..., n in start and finish positions, where

$$[W^j] = [\dot{A}^j][(A^j)^T], \quad \text{and} \quad \mathbf{v}^j = -[W^j]\mathbf{d}^j + \dot{\mathbf{d}}^j, \quad j = 1, \ldots, n. \qquad (20)$$

The dot denotes derivatives with respect to time. From this, the 4 x 4 spatial velocity matrix $[\Omega^j]$ is given by

$$[\Omega^j] = \begin{bmatrix} 0 & -w_{z,j} & w_{y,j} & v_{x,j} \\ w_{z,j} & 0 & -w_{x,j} & v_{y,j} \\ -w_{y,j} & w_{x,j} & 0 & v_{z,j} \\ 0 & 0 & 0 & 0 \end{bmatrix}, \qquad (21)$$

where $\mathbf{w}^j=(w_{x,j}, w_{y,j}, w_{z,j})$ is the angular velocity vector and $\mathbf{v}^j=(v_{x,j}, v_{y,j}, v_{z,j})$ is the linear velocity vector at the jth position. Assuming the acceleration properties of the motion are defined at the j-th position, yields to:

$$[\alpha^j] = [\dot{W}^j], \quad \text{and} \quad \mathbf{a}^j = \dot{\mathbf{v}}^j. \qquad (22)$$

In order to define the 4 x 4 acceleration matrix $[\Lambda^j]$, we introduce the 4 x 4 matrix constructed from (22), $[\dot{\Omega}^j]=[\alpha^j, \mathbf{a}^j]$, to obtain

$$[\Lambda^j] = [\dot{\Omega}^j] + [\Omega^j][\Omega^j], \qquad (23)$$

where j denotes the position in which the acceleration terms are defined.

Spatial Synthesis Applications

The spatial synthesis example is a part of the authors' efforts to explore new, efficient methods for the design of fault-tolerant robot manipulators, as well as novel task-planning techniques. Particularly, the authors examined a non-redundant general six-degree-of-freedom TRS robot manipulator (see Figure 2), mounted on a movable platform is fault-tolerant with respect to the originally specified task, consisting of second-order specifications, after one of its joints fails and is locked in place.

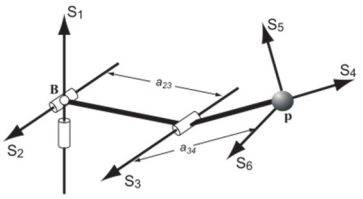

Figure 2. The TRS arm is a general six-degree of freedom serial chain configured so that the first pair of revolute joints intersect at right angles forming T-joint (also known as U-joint) and the last three joints intersect in a point to define a spherical wrist

The Dentavit-Hartenberg parameters [20] of the arm are listed in Table 1. The task data is presented in Table 2. It consists of two positions with velocity, defined in the first position and velocity and acceleration specifications in the second position.

Table 1. Denavit-Hartentberg parameters for the TRS arm

Link	$\alpha_{i-1,i}$	$a_{i-1,i}$	θ_i	d_i
1	—	—	θ_1	0
2	$\pi/2$	650 mm	θ_2	0
3	0	0	θ_3	650 mm
4	$\pi/2$	0	θ_4	0
5	$\pi/2$	0	θ_5	0
6	$\pi/2$	0	θ_6	0

Table 2. Task data for planning movement of the TRS arm

Data	Start Position	Finish Position
Position (rad; mm)	$(0, -\pi/2, \pi; 0, 0, -350)$	$(\pi, \pi/2, 0; 0, -100, -800)$
Velocity (rad/s; mm/s)	$(0, 100, -300; -10, -100, -100)$	$(-100, 0, 0; -100, 10, 0)$
Accel. (rad/s^2; mm/s^2)	–	$(0, 0, 0, -100, 10, 0)$

Figure 3 shows the TRS arm moving through the specified task. The trajectory is determined from the joint parameters using a fifth-degree polynomial interpolation following [21], [22].

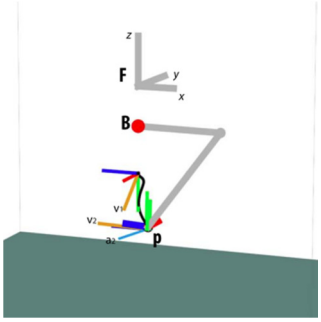

Figure 3. The world frame F, the location of fixed pivot B in the base of the arm, the moving pivot p of the TRS arm

In the following sections, the authors present the recovery strategy for the six-degree-of-freedom TRS arm, to achieve the originally specified task in the case of an actuator failure.

Arm Actuator Failures

The recovery strategy is based on the ability to reposition the arm base so that the point **B** at the intersection of S_1 and S_2 of the TRS can be placed where needed in a horizontal plane parallel to the X-Y plane of the world frame F. The point **B** lies at the origin of the fixed coordinate system, B_z = -140 mm at all times, i.e. the arm base can move freely in the X-Y plane. The authors assumed that the TRS arm could grasp the tool frame where necessary so that the wrist center **P** could be positioned in **F** where necessary. The proposed strategy reconfigures the arm-platform system using degrees of freedom that exist in the system but are locked during arm movement. Thus, the recovery plan is achieved by first identifying values for the reconfiguration parameters **B**=(B_x, B_y, -140) and **P**=(P_x, P_y, P_z) that ensure that the end-effector of the TRS arm can achieve the specified task for each particular arm joint failure, shown below. These constraint equations combine with the specified task to provide a set of polynomial equations for the reconfiguration parameters of the platform arm system. Solutions to these equations are obtained numerically using the polynomial homotopy continuation sofware PHC [23]. The movement of each reconfigured arm is determined by solving the inverse kinematics failure model in each of the task positions, and then using joint trajectory interpolation to guide its end-effector through the prescribed task [14].

Assume that the actuator of joint S_1, in Figure 2, which controls the shoulder azimuth angle, of the TRS arm has failed and that the brakes have been set to maintain a constant angle θ_1.The remaining actuated joints of the TRS form a parallel RRS chain that can position the wrist in a plane perpendicular to the horizontal axis. Once a normal **G**=(G_x, G_y, G_z) to this plane and a position of the wrist center **P**=(P_x, P_y, P_z) are identified, then the coordinates of the base pivot **B** can be computed to reposition the base of the platform to

allow the arm to guide the tool frame through the specified task, despite the S_1 joint failure [24]. The polynomial system of design equations for the parallel RRS consists of four bilinear quadratic equations and one linear equation in the five unknowns $\mathbf{r}=(G_x, G_y, P_x, P_y, P_z)$. The total degree of the system is $2^4 = 16$, which is small enough to directly eliminate the variables and obtain a univariate polynomial of degree six. The solution, corresponding to failure at $\theta_1 = 90^o$, is given in Table 3.

Table 3. The reconfiguration parameters for a failed S_1 joint

$\mathbf{B}=(B_x,B_y,B_z)$ (mm)	$\mathbf{P}=(P_x,P_y,P_z)$ (mm)
(0, 0, -140)	(0, -412.6, -487)

Figure 4(a) shows the reconfigured platform arm system and the trajectory generated to guide the TRS arm through the original task with an S_1 joint failure.

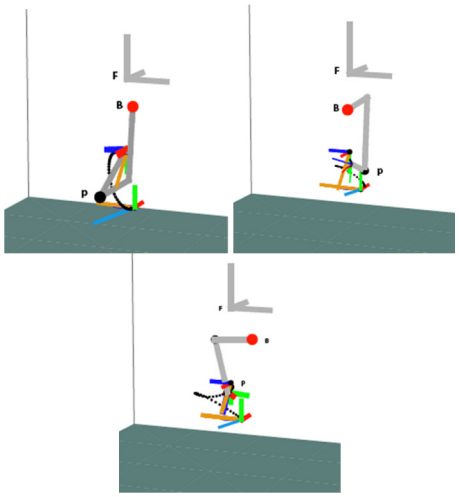

(a) (b) (c)

Figure 4. (a) The reconfigured platform arm system for an S_1 actuator failure. (b) The reconfigured platform arm system for an S_2 actuator failure. (c) The reconfigured platform arm system for an S_3 actuator failure

Next, the authors considered the case in which the actuator of the second joint S_2 of the TRS arm, which controls the shoulder elevation angle, fails and that the brakes have been set to maintain θ_2 at a constant value. The remaining joints of the arm in Figure 2 form a perpendicular RRS chain that can locate the wrist center on a circular torus. We obtain five polynomial equations that define the reconfiguration parameters $\mathbf{r}=(B_x, B_y, P_x, P_y, P_z)$ that allow the platform arm system to complete the task despite the failure. The system of five quartic polynomials has a total degree of $4^5 = 1024$. The real solution, corresponding to shoulder elevation failure at $\theta_2 = 0^o$, is listed in Table 4.

Table 4. The reconfiguration parameters for a failed S_2 joint

$\mathbf{B}=(B_x,B_y,B_z)$ (mm)	$\mathbf{P}=(P_x,P_y,P_z)$ (mm)	Bz^* (mm)
(62.31, -184.54, -140)	(21.19, 122.75, -466.16)	-140

Figure 4(b) shows the reconfigured rover arm system for the crippled TRS arm with an S_2 joint failure through the original task. If the elbow actuator of joint S_3 of the TRS arm in Figure 2 fails then we assume its brakes can be set so that θ_3 has a constant value. The remaining joints of the arm form a TS chain that can position the wrist center $\mathbf{p}=[\boldsymbol{K}_0^1]\mathbf{P}$ on a sphere, with a radius R, about the base point **B**. The radius R is defined by the link lengths a_{23} and a_{34}, the angle θ_3, and is equal to

$$R^2 = a_{23}^2 + a_{34}^2 - 2a_{23}a_{34}\cos\theta_3, \qquad (31)$$

where the value of θ_3 is determined from the joint sensor of the failed actuator. As in the previous cases, we seek the reconfiguration parameters $\mathbf{r}=(B_x, B_y, P_x, P_y, P_z)$ that allow the arm to perform the original task, despite the failure. The polynomial system consists of five quadratic equations in the unknowns **r** and has a total degree of $2^5 = 32$ [25]. The real solution, corresponding to elbow failure at $\theta_3 = 68.56^o$, i.e. R= 400 mm, is given in Table 5.

Table 5. The reconfiguration parameters for a failed S_3 joint

$\mathbf{B}=(B_x,B_y,B_z)$ (mm)	$\mathbf{P}=(P_x,P_y,P_z)$ (mm)	R (mm)
(17.1, -124, -140)	(-33.4, 158, 418)	400

Figure 4(c) shows the reconfigured platform-arm system and the trajectory generated to guide the TRS with the elbow joint failure to achieve the originally specified task. A Surface Mobility Platform (Gears LLC), a Lynxmotion robot arm, integrated using Single-Board RIO – 9632 (National Instruments) are used for the experimental set up. Tests of the proposed strategy are currently performed in the Space Robotics Lab at Texas A&M (see Figure 5).

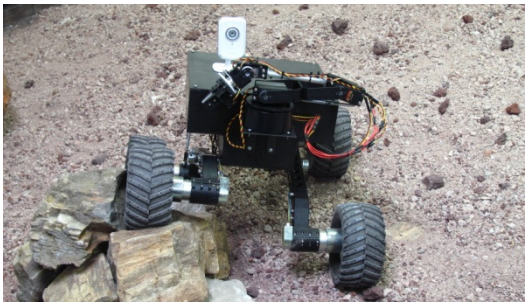

Figure 5. Experimental set up. Arm in stowed position

Figure 6 (a) shows the healthy arm holding a tool, moving through a task consisting of second-order specifications. Figure 6(b) shows the new location of the fixed **B** and moving **p** pivots of the arm, after an elbow failure. The closer

look shows how the re-grasping ability of the end-effector had allowed for the tool to be grasped at a different location.

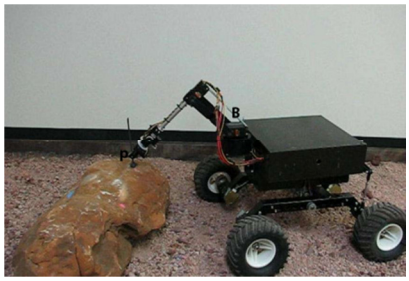

(a)

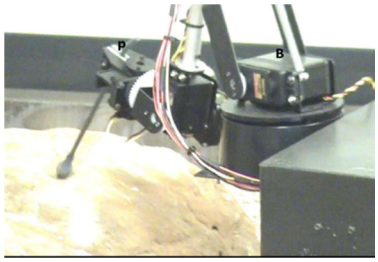

(b)

Figure 6. (a) The healthy arm moving through the a task. (b) New locations for the base pivot B and the moving pivot p have been obtained in order for the crippled TS arm to obtain the originally specified task despite the elbow failure

Finally, Figure 8 is a recent result from our efforts to design mechanical linkages, constrained to have the same coordinates for the fixed pivot **B** and the same end-effector path trajectory.

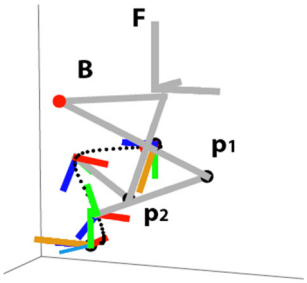

Figure 8. The TS chain (Bp1) and the perpendicular RRS chain (Bp2) move smoothly through the second order task

The animation shows that both TS and perpendicular RRS linkages satisfy the second-order task specification and move smoothly throughout the task.

Summary

Formulation of the kinematic specification for the synthesis of spatial kinematic chains with specified task acceleration was presented. Applications have focused on exploring new strategies for the failure recovery of general six-degree-of-freedom manipulators. The last example combines the second-order effects of the task with the particular kinematics of the chain to yield free parameters that allow for more than one system to accomplish the same task.

References

[1] D. Tesar and J. W. Sparks, "The Generalized Concept of Five Multiply Separated Positions in Coplanar Motion", *J. Mechanisms*, 1968, 3(1), 25-33.

[2] H. J, Dowler, J. Duffy, and D. Tesar, "A Generalised Study of Four and Five Multiply Separated Positions in Spherical Kinematics—II", *Mech. Mach. Theory*, 1978, 13:409-435.

[3] Chen P. and Roth B., "Design Equations for the Finitely and Infinitesimally Separated Position Synthesis of Binary Links and Combined Link Chains", *ASME Journal of Engineering for Industry*, 1969, Vol. 91: 209-219.

[4] Hanafusa H., and Asada H., "Stable Prehension by a Robot Hand with Elastic Fingers", *Proc. 7-th Int. Symp. Ind. Robots,* 1977, pp. 384-389.

[5] Cai, C.C., and Roth B., "On the Spatial Motion of a Rigid Body with a Point Contact", *IEEE Int. Conf. on Robotics and Automation*, 1987, pp. 686-695.

[6] Montana, D.J., "The Kinematics of Contact and Grasp", *Int. Journal Robot. Research*, 1988, vol. 7, N0. 3, pp. 17-25.

[7] Park, J., Chung W. and Youm Y., Second Order Contact Kinematics for Regular Contacts," *IEEE Conference on Intelligent Robots and Systems*, 2005, pp.1723-1729.

[8] Sarkar N., Yun S., and Kumar V., "Dynamic Control of 3D Rolling Contacts in Two Arm Manipulation", *IEEE Int. Conf. on Robotics and Automation*, 1993, pp. 978-983.

[9] Trinkle J.C., "On the Stability and Instantaneous Velocity of Grasped Frictionless Objects", *IEEE Trans. Robotics and Automation*, 1992, vol.8, pp. 560-572.

[10] Ohwovoriole M. S. and Roth B., "An Extension of Screw Theory", *J. Mech. Design*, 1981, Vol. 103. pp. 725-735.

[11] Reuleaux F., The Kinematics of Machinery, 1963, New York: Dover.

[12] Mishra B., Schwarz J.T., and Sharir M., "On the Existence and Synthesis of Multi-finger Positive Grips", *Algorithmica*, 1987, Vol. 2, pp. 541-558.

[13] Markenskoff X., Ni L. and Papadimitriou C.H., "The Geometry of Grasping", *Int. J. Robot. Research*, 1990, vol. 9,pp. 61-74.

[14] E. Rimon and Burdick J., "A Configuration Space Analysis of Bodies in Contact - I. 1-st Order Mobil-

ity", *Mechanism and Machine Theory*, 1995, Vol.30(6) : 897-912.
[15] E. Rimon and Burdick J., "A Configuration Space Analysis of Bodies in Contact - II. 2-nd Order Mobility", *Mechanism and Machine Theory*, 1995, Vol. 30(6): 913-928.
[16] N. Robson and McCarthy J. M., "Kinematic Synthesis with Contact Direction and Curvature Constraints on the Workpiece", *ASME Int. Design Engineering Conference,* 2007.
[17] N. Patarinsky Robson and J. M. McCarthy, "Synthesis of a Spatial SS Serial Chain for a Prescribed Acceleration Task", *Proc. IFToMM, The 12th World Congress on Mechanism and Machine Science*, June 18-21, 2007, Besancon, France.
[18] N. Patarinsky Robson, J. M. McCarthy and I. Tumer, "Applications of the Geometric Design of Mechanical Linkages with Task Acceleration Specifications*", ASME Int. Design Eng. Tech. Conf.*, 2009, August 30-Sept.2, San Diego, CA.
[19] McCarthy, J.M., Geometric Design of Linkages, Springer-Verlag, 2000, New York.
[20] Hartenberg, R. S., and Denavit, J., Kinematic Synthesis of Linkages, 1964, McGraw-Hill, New York.
[21] Craig, J., Introduction to Robotics, Mechanics and Control, 1989, Addison - Wesley Publishing Co.
[22] N. Patarinsky Robson, J. M. McCarthy and I. Tumer, 2009, "Exploring New Strategies for Failure Recovery of Crippled Robot Manipulators*", ASME/IFToMM Int. Conf. On Reconfigurable Mech. and Robots (ReMAR'09)*, June 22-24, London, UK.
[23] Verschelde, J., and Haegemans, A., "The GBQ-Algorithm for Constructing Start Systems of Homotopies for Polynomial Systems", *SIAM Soc. Ind. Appl. Math. J. Numer. Anal*., 1993, 30(2), pp. 583 – 594.
[24] N. Patarinsky Robson, J. M. McCarthy and I. Tumer, "Failure Recovery Planning for an Arm Mounted on an Exploratory Rover*",* 2009, *IEEE Transactions on Robotics,* 25(6), pp. 1448-1453.
[25] N. Patarinsky Robson, J. M. McCarthy and I. Tumer, "The Algebraic Synthesis of a Spatial TS Chain for a Prescribed Acceleration Task", *Mechanism and Machine Theory*, 2008, 43: pp.1268-1280.

Biographies

NINA ROBSON is an assistant professor in Manufacturing and Mechanical Engineering Technology at Texas A&M University. Her research is in robotics, kinematics of motion, and biomechanics. Her e-mail address is ninarobson@tamu.edu.

J. M. MCCARTHY is a professor in Mechanical Engineering at University of California, Irvine. His research is in design of mechanical systems, computer aided design, and kinematic theory of spatial motion. He can be reached at jmmccart@uci.edu.